Exergoeconomic Analysis of a Solar-Geothermal Hybrid Organic Rankine System

Fatih Akkurt*

Faculty of Engineering, Department of Energy Systems Engineering, Necmettin Erbakan University, Konya, Turkey

Abstract: In this study, energy, exergy and exergoeconomic analysis of a solar-geothermal hybrid Organic Rankine Cycle System with a nominal 50 [kW] turbine capacity was conducted at a range of 50-90 [°C] geothermal source temperatures in Konya, Turkey. A new generation R1234yf was assumed as the working fluid of the system. An average of 336 [MWh/year] annual electricity generation was obtained for all source temperatures, 8.1% of which was with solar energy effect. Exergy efficiencies were approximately 6.2% for all geothermal temperatures, while the energy efficiencies increased at a range of 4.3%-10.0% with the increase of geothermal source temperatures. Exergoeconomic analysis was performed with the SPECO method. According the exergoeconomic analysis results, electricity generation costs of the system were determined as 32.2, 38.8, 36.1, 36.5 and 37.8 [USD/MWh] with the increase of geothermal source temperature.

Keywords: Organic rankine cycle; Geothermal energy; Solar energy; Exergoeconomic analysis; SPECO method

1. Introduction

Due to the increasing demand of electricity in the world and the harmful effects of conventional electricity generation methods to the environment, electricity generation through renewable energy sources is becoming increasingly important. Geothermal energy has an important place among renewable energy sources in electricity generation. Geothermal sources are basically used for electricity generation with two different types of systems including flash and binary. Among geothermal energy sources, flash systems are suitable for high temperature sources > 220 [°C] while binary systems are suitable for medium and low temperature sources [1].

Turkey is ranked as the twelfth in geothermal energy capacity among the countries of the world. There are 1000 hot water and mineral water sources and geothermal wells in Turkey. Of these, 170 sources are at the temperatures above 40 [°C]. Such medium and low temperature sources are suitable for heating, industrial process and spa use [2]

Organic Rankine Cycle (ORC) is a cycle that can generate electricity at medium and low temperature energy sources such as solar energy, waste heat, biomass and geothermal energy. The availability of ORC with geothermal energy varies between 50-350 [°C] source temperatures. However, system efficiencies are not high for low temperature sources <100 [°C] [3].

Exergy analysis is an effective analysis method as a combination of the first and second laws of thermodynamics. Exergy is defined as the maximum work potential that can be obtained from the system according to the reference conditions. In the exergy analysis, the entropy production in a system is taken into account and it provides a more comprehensive analysis of the system. Besides, exergoeconomic analysis, as a combination of exergy analysis and economic principles, is a method that investigates the costs of system outputs and exergy destructions and helps in the systematic study and optimization of energy systems [4].

Determining the energy and exergy efficiencies and conducting their economic analysis of solar-geothermal hybrid systems have been the main targets for many researchers. A literature survey of energy, exergy and exergoeconomic analysis of a solar-geothermal hybrid systems was presented in Table 1.

In this study, energy, exergy and exergoeconomic analysis of a solar-geothermal hybrid ORC system with an optimum 50 [kW] turbine capacity was investigated between 50-90°C geothermal source temperature. R1234yf was assumed to be the working fluid of the system. Component capacities of the system

were determined according to night and daytime working conditions of the system. The annual electricity generation, energy and exergy values of the system were obtained with EES and EXCEL program using hourly climatic conditions in Konya, Turkey [17].

Exergoeconomic analysis was performed with the SPECO method. In most of cases studied for the hybrid solar-geothermal system, the geothermal temperatures are ranged from 150 to 200 [°C] However, few studies have examined the thermal-economic feasibility of hybrid systems in different regions, especially where geothermal water temperatures are below 100 [°C] [15]. Moreover, in many studies, the results were determined according to the parameters such as solar irradiation and environmental temperature that kept constant or ranged at some values. An important novelty of this study is that the calculations were conducted for the solar irradiation and environmental temperature values of for each hour of the year and the annual energy, exergy and exergoeconomic results were obtained by the sum of all year data. This study was conducted to provide guidance for such hybrid ORC systems that considered to be installed where geothermal water temperatures are below 100 [°C'] which are more common in the world.

2. System description

The scheme of the solar-geothermal hybrid ORC system and T-s diagrams of the system regarding night and daytime operating conditions were presented in Figure 1. The system mainly consists of evaporator, turbine-generator subsystem, heat exchanger-collector subsystem, condenser and pump.

The system works only with geothermal energy at night working conditions. Geothermal fluid enters the evaporator at state 1 and leaves its heat to the working fluid, then is injected to the geothermal well at state 2. The working fluid enters the evaporator as saturated liquid at state 4 and exits the evaporator as saturated steam at state 5 to enter the turbine. It leaves from turbine at state 6 and enters to condenser. In the condenser, the working fluid leaves its heat to the cooling water entering the condenser at state 7 and exits the condenser as saturated liquid at state 3. Cooling water leaves the condenser at state 8. After the working fluid exits from the condenser at state 3, its pressure increases in the pump and enters the evaporator at state 4.

In the daytime, different from the night conditions, the fluid coming out of the evaporator was assumed to be directed to the heat exchanger thanks to sun sensitive controlled valve. With the effect of the additional solar energy, working fluid enters the turbine as superheated steam at state 9. It then returns to the evaporator in a process like nighttime conditions. On the other hand, the cooling water enters the condenser at state 7 and exits at state 11. In the collector-heat exchanger subsystem, water enters the heat exchanger at state 13 and returns to the collector at state 12.

3. Design parameters

General equation of the first law of thermodynamics implemented as Eq. (1) for system components to determine the component capacities of the system for optimum 50 kW turbine capacity.

$$\dot{Q} - \dot{W} = \dot{m} \cdot \left(h_{out} - h_{in} \right) \tag{1}$$

where, $\dot{Q}, \dot{W}$, $\dot{m}$, h_{out} and h_{in} are the heat transfer rate, work, the fluid flow rate and specific enthalpy of the outlet and inlet fluids of the component, respectively.

Evaporator, condenser, and pump capacities were calculated based on the nighttime working conditions. Turbine and heat exchanger capacities, collector fluid rate and collector area of the system were determined according to the maximum atmospheric condition in a year when the solar radiation and ambient temperature were 1 [kW/m^2] and 30[°C], respectively. Some assumptions in the calculations were presented below:

- The pinch point temperatures in the evaporator and condenser between states (a-b and c-d) were accepted as 3 [°C] [18].
- The temperature differences between states 5-1 in evaporator and states 3-7 in condenser were accepted as 5 [°C] [18].
- The inlet temperature of the cooling water to the condenser at state 7 was accepted as 20 [°C].
- The maximum inlet temperature of the working fluid to the turbine was accepted as 120 [°C].
- The temperature differences between state 12-5 and state 13-9 in collector were accepted as 5 [°C].

The design parameters were obtained and presented in Table 2 for each geothermal source temperature.

4. System analysis

4.1 Energy analysis

Energy analysis of a solar-geothermal hybrid Organic Rankine Cycle was investigated for geothermal source at a range of 50-90 [°C] geothermal source temperature. The night performance of the system changes with only geothermal source temperature, while the daytime performances changes both with hourly solar conditions and geothermal source temperature. The heat input to the system $\dot{Q}_{in}$ was calculated, as the sum of the heat obtained from the solar collectors $\dot{Q}_{solar}$ and evaporator $\dot{Q}_{evap}$ with the Eq. (2).

$$\dot{Q}_{in} = \dot{Q}_{evap} + \dot{Q}_{solar} \qquad (2)$$

For the night working conditions, this equation corresponds only to the heat obtained from the evaporator. The collector efficiency η_{coll} and the solar energy input to the system $\dot{Q}_{solar}$ were calculated using hourly average solar radiations and ambient temperatures of all year with the Eq. (3-4) respectively.

$$\eta_{coll} = 0.8 - 1.5 \cdot \left(\frac{T_{12} - T_{amb}}{I} \right) \qquad (3)$$

$$\dot{Q}_{solar} = A_{coll} \cdot I \cdot \eta_{coll} \qquad (4)$$

where, T_{amb}, I and A_{coll} are the hourly average ambient temperature, hourly average solar irradiation and collector area, respectively. The work of turbine at night condition $W_{turb,night}$ was calculated with Eq. (5).

$$\dot{W}_{turb,night} = m_r \cdot \left(h_5 - h_6 \right) \qquad (5)$$

where, m_r is the mass flow rate of the refrigerant. Turbine inlet condition state 9 according to $\dot{Q}_{in}$ for the environmental conditions of each hour of the day determined with Eq. (6).

$$\dot{Q}_{in} = m_r \cdot \left(h_9 - h_5 \right) \qquad (6)$$

Afterwards, the turbine work $\dot{W}_{turb,daytime}$ and pump work $\dot{W}_{pump}$ was calculated with the Eq. (7-8) respectively.

$$\dot{W}_{turb,daytime} = m_r \cdot \left(h_9 - h_{10} \right) \qquad (7)$$

$$\dot{W}_{pump} = m_r \cdot \left(h_4 - h_3 \right) \qquad (8)$$

The electricity generation $\dot{EG}$ of the system in any hour was calculated with Eq. (9).

$$EG = \eta_{turb-gen} \cdot \dot{W}_{turb} - \eta_{pump} \cdot \dot{W}_{pump} \qquad (9)$$

where, $\eta_{turb-gen}$ and η_{pump} are the efficiencies of turbine-generator combination and pump, respectively. The efficiencies of turbine-generator combination and pump were taken as 81% and 80% respectively. The annual energy efficiency of the system $\eta_{sys,annual}$ was calculated according to the ratio of electricity generation to heat inputs as sum of all days of the year with Eq. (10).

$$\eta_{sys,annual} = \frac{\sum_{d=1}^{d=365} \dot{E}G}{\sum_{d=1}^{d=365} \dot{Q}_{in}} \qquad (10)$$

4.2 Exergy analysis

The exergy value of the any system point $\dot{E}x_x$ was calculated with Eq. (11) as the general exergy the equation.

$$\dot{E}x_x = \dot{m}_x \cdot \left[\left(h_x - h_0 \right) - T_0 \cdot \left(s_x - s_0 \right) \right] \qquad (11)$$

where, $\dot{m}_x$, h_x and h_0, s_x and s_0 are the fluid flow rate, specific enthalpy and entropy of the fluid at system point and reference condition, respectively. The reference condition was accepted to be P_0=100 [kPA] and T_0=20 [°C] for all kind of fluids. The exergy inputs to the system $\dot{E}x_{in}$ were calculated as the sum of geothermal exergy at state 1 $\dot{E}x_1$ and solar exergy $\dot{E}x_{solar}$ with Eq. (12).

$$\dot{E}x_{in} = \dot{E}x_1 + \dot{E}x_{solar} \qquad (12)$$

The solar exergy input to the system $\dot{E}x_{solar}$ was calculated with Eq. (13) suggested by [19].

$$\dot{E}x_{solar} = A_{coll} \cdot I \cdot \left[1 + \frac{1}{3} \cdot \left(\frac{T_0}{T_{sun}} \right)^4 - \frac{4}{3} \cdot \left(\frac{T_0}{T_{sun}} \right) \right] \quad (13)$$

where, T_{sun} is the sun temperature accepted as 6000 [°K]. The exergy input to the system was only with geothermal source for night working conditions. The annual exergy efficiencies of system $\psi_{sys,annual}$ was calculated according to the ratio of exergy to heat inputs as sum of all days of the year with Eq. (14).

$$\psi_{sys,annual} = \frac{\sum_{d=1}^{d=365} \dot{E}G}{\sum_{d=1}^{d=365} \dot{E}x_{in}} \quad (14)$$

As well as the general exergy efficiency of the system, it is important to know the exergy efficiencies of system components at a design point of view. For this purpose, exergy efficiency of each component ε_k was calculated according to the fuel-product approach with Eq. (15).

$$\varepsilon_k = \frac{\dot{E}x_{P,k}}{\dot{E}x_{F,k}} \quad (15)$$

where, $\dot{E}x_{P,k}$ and $\dot{E}x_{F,k}$ are the product and fuel exergy of the system component, respectively. Besides, fuel, product, and exergy destruction of system components were determined with the equations presented in Table 3.

4.3 Exergoeconomic analysis

In this study, specific exergy costing (SPECO) method which was created as a combination of exergy analysis and economic principles, was used for the exergoeconomic analysis of the [20]. For this purpose, initial investment cost values of each component were determined with the equations given in Table 4.

The general cost balance of each component was created with Eq. (16).

$$\sum \dot{C}_{in,k} + \dot{C}_{q,k} + \dot{Z}_k = \sum \dot{C}_{out,k} + \dot{C}_{w,k} \quad (16)$$

where, $\sum \dot{C}_{in,k}$, $\sum \dot{C}_{out,k}$, $\dot{C}_{q,k}$ and $\dot{C}_{w,k}$ are the inlet, outlet, heat and work exergy costs, respectively and $\dot{Z}_k$ is annual investment rates of each component. The exergy cost of the flow was determined with Eq. (17).

$$\dot{C}_k = c \cdot \dot{E}x \quad (17)$$

where, c and $\dot{E}x$ are the unit exergy cost and exergy of system point. Annual investment rates of a components $\dot{Z}_k$ were calculated with Eq. (18) with the use of Z_k, CRF and ϕ were initial investment cost, capital recovery and maintenance factors, respectively.

$$\dot{Z}_k = Z_k \cdot CRF \cdot \phi \quad (18)$$

where, ϕ and CRF are the maintenance factor, annual working hours and capital recovery factor of the component, respectively. The maintenance factor was assumed as 1.06. Capital recovery factor was determined with Eq. (19).

$$CRF = \frac{i \cdot (i-1)^n}{(i-1)^n - 1} \quad (19)$$

where, i and n are the annual interest rate and economic lifespan of the system, respectively. The annual interest rate and economic lifespan of the system were assumed 0.1 and 20 years, respectively.

The exergy destruction cost rates $\dot{C}_{D,k}$ which occur due to the irreversibility of the system components were calculated with Eq. (20).

$$\dot{C}_{D,k} = c_{f,k} \cdot \dot{E}x_{D,k} \quad (20)$$

where, $c_{f,k}$ and $\dot{E}x_{D,k}$ were the average cost per unit fuel exergy and exergy destruction of the component, respectively. The average unit fuel exergy cost was calculated with Eq. (21).

$$c_{f,k} = \frac{\dot{C}_{F,k}}{\dot{E}x_{F,k}} \quad (21)$$

where, $\dot{C}_{F,k}$ and $\dot{E}x_{F,k}$ are the fuel exergy cost and fuel exergy of the component, respectively. The cost performance of a system component depends both on investment rate and the exergy destruction cost of the system component. This expression is defined as the exergoeconomic factor f_k and was obtained for the components as follows as the ratio of the annual investment rate to the sum of the investment rate and the exergy destruction cost [21]. It is calculated with Eq. (22).

$$f_k = \frac{\dot{Z}_k}{\dot{Z}_k + \dot{C}_{D,k}} \qquad (22)$$

The range of exergoeconomic factor is from 0 to 1. If the exergoeconomic factor is close to 0, the cost of irreversibility predominates on component. Else, the cost of investment has a greater effect [22].

All cost balance equations and auxiliary equations were presented in Table 5. If "n" number of flow exergies come out of a system component while it has only one the cost balance equation, "n-1" auxiliary equations are needed [22]. Therefore, some auxiliary equations including the boundary conditions of the incoming flows were used for the solutions. Of these, specific cost of the incoming solar energy, geothermal water and cooling water c_{solar}, c_1 and c_7 were assumed as zero.

5. Results and discussion

5.1 Energy and exergy

The variation of annual electricity generation with geothermal and solar energy and their percentages were presented in Figure 2 with the increase of geothermal source temperature. The electricity generation values were determined close to each other for all source temperatures. The annual electricity generation of the system was approximately 336 MWh for all temperatures and the effect of solar energy is determined as 8.1% on average. Although, operating temperatures and enthalpy values increase, the decrease of fluid flow rates caused electricity generation to be close to each other for all source temperatures. In addition, the fact that the operating temperatures and enthalpy values are close to each other, despite the decrease in the collector area, caused the effect of solar energy on the annual electricity production to be close to each other.

The variation of annual energy and exergy efficiency values of the system with the increase of geothermal source temperature were presented in Figure 3. Energy efficiency values increased with the increase of the geothermal source temperature and calculated as 4.3%, 6.0%, 7.5%, 8.9% and 10.0%, respectively. Because the energy input to the system decreased because of the decreasing both the geothermal water and working fluid flow rates while the annual electricity generation were close to each other. The exergy efficiency values followed approximately 6.2% with the increase of geothermal temperature according to the reason of constant annual and exergy inputs and close annual electricity generations. The reason of constant exergy input for every geothermal source temperature were decreasing the geothermal water flow rates and increasing temperature difference between the geothermal water and the reference condition with the increase of geothermal source temperature.

The variation of the annual exergy destructions of the system components with the increase of geothermal source temperature were presented in Figure 4. Maximum exergy destruction occurred in collectors. Evaporator, turbine, condenser, pump and heat exchanger followed the collectors. The annual exergy destructions increased for collectors, condenser and heat exchanger while exergy destructions were constant for evaporator and turbine with the increase of geothermal temperature. The annual exergy destruction values of collectors, condenser and heat exchanger decreased at the range of 907-272 [MWh], 109-47 [MWh] and 10-4 [MWh], respectively. Annual exergy destructions of evaporator and turbine slightly increased at a range of 11. 6-13.6 [MWh] and 86-88 [MWh], respectively. For the pump, exergy destruction was 12 [MWh], at 50 [°C], then slightly decreased to a minimum value of 7 [MWh], at 70 [°C]. Later, it increased to 9 [MWh] at 90 [°C].

The variation of the exergy efficiencies of the system components with the increase of geothermal source temperature were presented in Figure 5. In general, exergy efficiencies remained approximately constant with the increase of geothermal source temperature except for the collectors. Average exergy efficiency of the system components determined as 80.8%, 72.8%, 16.4%, 80.6% and 92.8%, for evaporator, turbine, condenser, pump and heat exchanger, respectively. The

reason for this was that the fuel and product exergies of the system were proportionally constant for the mentioned components. For the collectors the exergy efficiency increased with the increase geothermal source temperature at a range of 17.5-51.1%. The increase in the exergy efficiency of the collectors was due to the decrease in the solar exergy input with decrease of collector area.

5.2 Exergoeconomy

The variation of exergy destruction cost rates of each system component with the increase of geothermal source temperature were presented in Figure 6. The annual exergy destruction cost rates were determined for all components as a function of the fuel cost and exergy destruction of the component. Exergy destruction cost rates of condenser decreased with the increase of geothermal source temperature and determined at a range of 2205-558 [USD/year]. That was because that the effect of exergy destruction was rather than fuel cost. The exergy destruction costs of both turbine and pump were determined 1501 and 490 [USD/year] at 50 [°C], respectively. They reached their lowest values of 1004 and 221 [USD/year] at 70 [°C]. Then they increased to 1156 and 343 [USD/year] at 90 [°C]. For turbine, the effect of exergy destruction on cost rates were greater than effect of fuel cost but for the pump their effects were same. Although exergy destruction decreased for collectors with the increase of geothermal source temperature, the increase of fuel costs caused an increase on exergy destruction cost rates and determined at the range of 1473-1854 [USD/year]. For the heat exchanger, the decrease of both exergy destruction and fuel costs caused the exergy destruction costs to decrease and determined at the range of 236-58 [USD]. For the evaporator, exergy destruction costs were zero for all geothermal source temperatures because of its zero-fuel cost.

The variation of exergoeconomic factors of each system component with the increase of geothermal source temperature were presented in Figure 7. The exergoeconomic factor of the evaporator determined as 1 for all geothermal source temperatures. Because the cost performance of evaporator depends only on the annual investment rate since the exergy destruction cost is zero. Exergy destruction costs of heat exchanger, turbine and pump were determined to be less than annual investment rates. So, the exergoeconomic factor of the heat exchanger increased at a range of 0.69-0.88. For the turbine and pump, exergoeconomic factors were as 0.85-0.78 at 50 [°C], then slightly reached to a maximum value of 0.89-0.82 at 70 [°C]. Later it slightly decreased to 0.88-0.81 at 90 [°C]. As the exergy destruction costs in the condenser decreased more than the annual investment rates with the increase of geothermal source temperature, exergoeconomic factor increased at the range of 0.24-0.46. The collector areas decreased with the increase of geothermal source temperature, so the annual investment rates have also decreased. Therefore, the exergoeconomic factor of collectors decreased at a range of 0.65-0.32, as the effect of the annual investment rates were more than the exergy destruction costs.

The variation of electricity generation costs with the increase of geothermal source temperature were presented in Figure 8. The electricity generation cost of the system was determined as 42.2, 38.8, 36.1, 36.5 and 37.8 [USD/MWh] at the range of 50-90 [°C], respectively. As the capacities and prices of system components decreased with the increase of the geothermal source temperature the electricity generation cost decreased until 70 [°C]. After to mentioned temperature, because of the increase in the pump capacity and accordingly its initial investment cost, electricity generation cost slightly increased.

5.3 Comparison of present study with literature survey

The result list of similar exergoeconomic analysis studies in the literature survey was presented in Table 6. The second law of thermodynamics deals with the quality of energy. As the source temperature increases, the quality of the energy also increases. Since systems containing ORC are operated with low-temperature energy sources, their efficiency is generally low. The most similar study in terms of source temperature, climate and system structure is the study conducted by [7]. Their energy efficiency at a range of 2.19-6.92% is approximately consistent with the current study's energy efficiency at a range of 4.3-10.0%. In the current study, the increase in energy efficiency with increasing source temperature is a requirement of the second law of thermodynamics. The differences of the current study with other studies in terms of

exergy efficiency can be explained with the differences in analysis methods and use of data.

The general conclusion obtained from all studies is that hybridization of the geothermal system with solar energy increases electricity production and system efficiency and reduces the cost of electricity. The improvement of approximately 8% by solar energy in the current study is approximately similar with the 5.5% and 6.3% improvement rates obtained by Ayub et al. (2015). Unit electricity cost is a result that varies depending on the complexity of the system. While this value decreases in simple systems, it may increase in more complex systems. In the literature survey, unit electricity cost varies at a range of 50-450 $/MWh. The electricity cost values in the range of 31.6-42.2 $/MWh obtained in the current study seem reasonable considering the simplicity of the system.

6. Conclusions

Energy, exergy and exergoeconomic analysis of a solar-geothermal hybrid ORC investigated at a range of 50-90 [°C] according to the climatic conditions in Konya, Turkey. A new generation R1234yf was selected as working fluid of the system. Optimum 50 [kW] turbine capacity was assumed for every geothermal source temperature. Exergoeconomic analysis was performed with the SPECO method. Some key outputs obtained from the calculations are listed below:

- An average 336 [MWh/year], electricity generation was obtained for all temperatures.
- Approximately 8.1% of electricity generation was obtained due to the solar energy for all source temperatures.
- The energy efficiencies increased at a range of 4.3-10.0% with the increase of geothermal source temperature.
- The exergy efficiencies were calculated as approximately 6.2% for all temperatures,
- Maximum exergy destruction occurred in collectors that is followed by evaporator, turbine, condenser, pump and heat exchanger.
- The electricity generation costs were determined as 42.2, 38.8, 36.1, 36.5 and 37.8 [USD/MWh] at a range of 50-90 [°C], respectively.

As a result, it has been concluded that such hybrid ORC systems, despite their low efficiency, can be installed to meet the electrical needs of facilities such as spas and greenhouses where low-temperature geothermal resources are used. It was understood that the support of geothermal energy used ORC systems with solar energy can contribute at a satisfactory rate on electricity generation.

Conflict of interest

The author declares that he has no conflict of interest with anyone.

References

1. Shengjun, Z., Huaixin W. and Tao G. ‘‘Performance comparison and parametric optimization of subcritical Organic Rankine Cycle (ORC) and transcritical power cycle system for low-temperature geothermal power generation’’, *Applied Energy*, **88** (2), pp. 2740–2754 (2011). DOI: 10.1016/j.apenergy.2011.02.034.

2. Kılıç, F.C. and Kılıç M.K. ‘‘Jeotermal Enerji ve Türkiye’’, *Mühendis ve Makina*, **54** (639), pp. 45-56 (2013).

3. Tchanche, B.F., Lambrinos G., Frangoudakis A., et al. ‘‘Exergy analysis of micro-organic Rankine power cycles for a small scale solar driven reverse osmosis desalination system’’, *Applied Energy*, **87** (4), pp. 1295–1306 (2010). DOI: 10.1016/j.apenergy.2009.07.011.

4. Nami, H., Mahmoudi S.M.S. and Nemati A. ‘‘Exergy, economic and environmental impact assessment and optimization of a novel cogeneration system including a gas turbine, a supercritical CO2 and an Organic Rankine Cycle (GT-HRSG/SCO2)’’, *Applied Thermal Engineering*, **110**, pp. 1315–1330 (2017). DOI: 10.1016/j.applthermaleng.2016.08.197.

5. Zhou, C., Doroodchi E. and Moghtaderi B. ‘‘An in-depth assessment of hybrid solar-geothermal power generation’’, Energy Conversion and Management, 74, pp. 88-101 (2013). DOI: 10.1016/j.enconman.2013.05.014.

6. Ayub, M., Mitsos A. and Ghasemi H., ‘‘Thermo-economic analysis of a hybrid solar-binary geothermal power plant’’, Energy, 87, pp. 326-335 (2015). DOI: 10.1016/j.energy.2015.04.106

7. Atiz, A., Karakilcik H., Erden M., et al. ‘‘Investigation energy, exergy and electricity production performance of an integrated system based on a low-temperature geothermal resource and solar energy’’, *Energy Conversion and Management*, **195**, pp. 798–809 (2019). DOI: 10.1016/j.enconman.2019.05.056.
8. Alibaba M., Pourdarbani R., Manesh M.H.K., et al. ‘‘Thermodynamic, exergo-economic and exergo-environmental analysis of hybrid geothermal-solar power plant based on ORC cycle using emergy concept’’, *Heliyon*, **6** (4), (2020). DOI: 10.1016 /j.heliyon .2020.e03758.
9. Başoğul Y., ‘‘A parametric study on exergoeconomic analysis for a binary geothermal power plant with ORC’’, *International Journal of Green Energy*, **18** (11), pp. 1117-1128 (2021). DOI: 10.1080/15435075.2021.1891910.
10. Tozlu, A., Gençaslan B. and Özcan H. ‘‘Thermoeconomic analysis of a hybrid cogeneration plant with use of near-surface geothermal sources in Turkey’’, *Renewable Energy*, **176**, pp. 237-250 (2021). DOI: 10.1016/j.renene.2021.05.064.
11. Sen, O. and Yılmaz, C. ‘‘Thermoeconomic analysis of a geothermal and solar assisted combined organic Rankine and absorption cycle’’, *International Advanced Researches and Engineering Journal*, **6** (1), pp. 34-42, (2022). DOI: 10.35860/iarej.1014569.
12. Guler O. F., Sen O., Yilmaz C. and Kanoglu M., ‘‘Performance evaluation of a geothermal and solar-based multigeneration system and comparison with alternative case studies: Energy, exergy, and exergoeconomic aspects’’, *Renewable Energy*, **200**, pp. 1517-1532 (2022). DOI: 10.1016/j.renene.2022.10.064.
13. Manesh, M. K., Rabeti, S. M., Nourpour, M., et al. ‘‘Energy, exergy, exergoeconomic, and exergoenvironmental analysis of an innovative solar-geothermal-gas driven polygeneration system for combined power, hydrogen, hot water, and freshwater production’’, *Sustainable Energy Technologies and Assessments*, **51**, 101861 (2022). DOI: 10.1016/j.seta.2021.101861.
14. Maali R. and Khir T. ‘‘Thermodynamic analysis and optimization of an ORC hybrid geothermal–solar power plant’’, *Euro-Mediterranean Journal for Environmental Integration*, **8**, pp. 341–352, (2023). DOI:10.1007/s41207-023-00359-1.
15. Li, D., Rao, Z., Zhuo, Q., et al. ‘‘Resource endowments effects on thermal-economic efficiency of ORC-based hybrid solar-geothermal system’’, *Case Studies in Thermal Engineering*, **52**, 103739 (2023). DOI: 10.1016/j.csite.2023.103739.
16. Mohammadi, M., Mahmoudan, A., Nojedehi, P., et al. ‘‘Thermo-economic assessment and optimization of a multigeneration system powered by geothermal and solar energy’’, *Applied Thermal Engineering*, **230**, 120656 (2023). DOI: 10.1016/j.applthermaleng.2023.120656.
17. Photovoltaic Geographical Information System, https://ec.europa.eu/jrc/en/pvgis, Accessed 20 July 2021, Subject: Solar radiation values.
18. Jankowski, M., Borsukiewicz A., Szopik-Depczyńska K., et al. ‘‘Determination of an optimal pinch point temperature difference interval in ORC power plant using multi-objective approach’’, *Journal of Cleaner Production*, **217**, pp. 798-807 (2019). DOI: 10.1016/j.jclepro.2019.01.250.
19. Petela, R. ‘‘Exergy of heat radiation’’, *ASME J. Heat Transfer*, **86** (2), pp. 187–192 (1964), DOI: 10.1115/1.3687092.
20. Lazaretto, A. and Tsatsaronis G. ‘‘SPECO: A systematic and general methodology for calculating efficiencies and costs in thermal systems’’, *Energy*, **31** (8-9), pp. 1257-1289 (2006), DOI: 10.1016/j.energy.2005.03.011.
21. Bejan, A., Tsatsaronis G. and Moran M.J. ‘‘Thermal design and optimization’’, Hoboken, New Jersey, John Wiley & Sons (1995).
22. Abuşoğlu, A. and Kanoğlu M. ‘‘Exergetic and thermoeconomic analyses of diesel engine powered cogeneration: Part1 – Formulations’’, *Applied Thermal Engineering*, **29** (2-3), pp. 234-241 (2008). DOI: 10.1016/j.applthermaleng.2008.02.025.

Table List

Table 1. A literature survey of energy, exergy and exergoeconomic analysis of a solar- geothermal hybrid systems.

Autor(s)	Product(s)	Source Temperature	Subject of the study
Zhou et al. [5]	•Electricity	90-210 °C	An energy and exergy analysis of hybrid solar–geothermal power plants where binary ORC geothermal plants are employed as part of system. The performances of the hybrid systems in terms of power output and the cost of electricity were compared with that of stand-alone solar and geothermal plants.
Ayub et al. [6]	• Electricity	135 °C	A performance analysis of a hybrid system consists of an ORC utilizing a low-temperature geothermal brine and a solar trough system. The performance of the hybrid system is optimized to maximize net power of the hybrid system. In a year-long operation, the performance of this hybrid system is assessed and compared with the performance of a sole geothermal system.
Atiz et al. [7]	• Electricity	63-74-86 °C	An energy, exergy and electricity generation analysis of a hybrid geothermal-solar ORC system three locations in Turkey with three different fluids.
Alibaba et al. [8]	• Electricity	150 °C	Thermodynamic, exergoeconomic and exergo-environmental analysis of hybrid geothermal-solar power plant based on ORC cycle using emergy concept in Tunisia.
Başoğul [9]	•Electricity	160-170 °C	The exergoeconomic assessment of a binary geothermal power plant (GPP) with organic Rankine cycle (ORC) is researched. A parametric study about the effect of well head and ambient temperatures, electricity production, and CO_2 release is conducted for the GPP.
Tozlu et al. [10]	•Electricity •Heating	100 °C	Thermodynamic and thermoeconomic analyses of three different configurations that the organic Rankine cycle (ORC), cogeneration system (CGN) and hybrid system (HYB), are coupled to the parabolic trough collector (PTC) system were carried out. For a case study a geothermal source located in the Kızılcahamam area of Ankara, as well as its solar data, are taken as reference for the hybrid system.

Sen and Yılmaz [11]	•Electricity • Cooling	130 °C	A geothermal and solar-assisted combined system is designed for the electricity and cooling of residences for geothermal and solar energy values of Afyonkarahisar city. An absorption cooling cycle was use for cooling purpose, while ORC use for electricity generation.
Guler et al. [12]	•Electricity • Heating • H_2 Production	130 °C	A performance analyze of a geothermal and solar-based multigeneration system for three different models ORC was used for electricity generation. The difference between model 1and 2 was of working fluid of ORC while difference between model 2 and the model 3 was the type of solar collector. The geothermal and solar energy values of Afyonkarahisar city were used.
Manesh et al [13]	•Electricity • Heating • H_2 Production • Fresh Water Production	150 °C	(4E) analyses of an innovative solar-geothermal-natural gas-driven polygenration system with ORC producing power, hydrogen, hot water, and freshwater.
Maali and Khir [14]	• Electricity	55–75 °C,	Energy and exergy analysis is conducted on a hybrid (solar–geothermal) organic Rankine cycle (ORC) power plant. The proposed system is designed to be installed in southern Tunisia. A parametric study is conducted for two typical days in summer and winter.
Li et al. [15]	• Electricity	70-90 °C	Thermo-economic examination of a 300 kW ORC-based hybrid solar-geothermal power generation system at four sites in China. The system utilizes geothermal water for preheating the organic working fluid and solar energy for superheating.
Mohammadi et al [16]	• Electricity • Heating • Cooling • Fresh Water Production	125-165 °C	Energy, exergy, and exergoeconomic analyses were applied for an innovative multigeneration system utilizing geothermal and solar energy sources for producing heating load, cooling load, electricity, and freshwater has been proposed. The system consists of two ORC and one SRC systems for electricity generation.

Table 2. Design parameters of the system.

T_1 [^oC]	Q_{evap} [kW]	A_{evap} [m^2]	Q_{cond} [kW]	A_{cond} [m^2]	Q_{HEX} [kW]	A_{HEX} [m^2]	A_{coll} [m^2]	W_p [kW]	W_{tmax} [kW]
50	801	108	771	115	436	81	567	6.7	50
60	581	96	547	92	280	65	371	4.7	50
70	471	84	435	81	202	57	263	3.8	50
80	404	77	369	74	156	52	215	4.5	50
90	356	73	322	69	128	49	180	5.3	50

Table 3. Fuel, product, and destruction exergy equations of components.

Component	Fuel exergy	Product exergy	Exergy destruction
Collector	$\dot{E}x_1 + \dot{E}x_{solar}$	$\dot{E}x_{13}$	$\dot{E}x_{D,coll} = \dot{E}x_{12} + \dot{E}x_{solar} - \dot{E}x_{13}$
HEX	$\dot{E}x_{13} - \dot{E}x_{12}$	$\dot{E}x_9 - \dot{E}x_5$	$\dot{E}x_{D,HEX} = \dot{E}x_{13} - \dot{E}x_{12} - \dot{E}x_9 + \dot{E}x_5$
Evaporator	$\dot{E}x_1 - \dot{E}x_2$	$\dot{E}x_5 - \dot{E}x_4$	$\dot{E}x_{D,evap} = \dot{E}x_1 - \dot{E}x_2 - \dot{E}x_5 + \dot{E}x_4$
Turbine	$\dot{E}x_9 - \dot{E}x_{10}$	$\dot{W}_{turb}$	$\dot{E}x_{D,turb} = \dot{E}x_9 - \dot{E}x_{10} - \dot{W}_{turb}$
Condenser	$\dot{E}x_{10} - \dot{E}x_3$	$\dot{E}x_{11} - \dot{E}x_7$	$\dot{E}x_{D,cond} = \dot{E}x_{10} - \dot{E}x_3 - \dot{E}x_{11} + \dot{E}x_7$
Pump	$\dot{W}_{pump}$	$\dot{E}x_4 - \dot{E}x_3$	$\dot{E}x_{D,pump} = \dot{W}_{pump} - \dot{E}x_4 - \dot{E}x_3$

Table 4. Initial investment cost values of the components of the system.

Component	Equation		Ref
Collector	$Z_{coll} = 38.8 \cdot A_{coll}$	[USD]	
HEX	$Z_{HEX} = 130 \cdot \left(\frac{A_{HEX}}{0.93} \right)^{0.78}$	[USD]	Tozlu et al. (2021)
Evaporator	$Z_{evap} = 130 \cdot \left(\frac{A_{evap}}{0.93} \right)^{0.78}$	[USD]	Tozlu et al. (2021)
Turbine	$Z_{turb} = 4405 \cdot \dot{W}_{turb}^{0.71}$	[USD]	Tozlu et al. (2021)
Condenser	$Z_{cond} = 130 \cdot \left(\frac{A_{cond}}{0.93} \right)^{0.78}$	[USD]	
Pump	$Z_{pump} = 3540 \cdot \dot{W}_{pump}^{0.71}$	[USD]	Tozlu et al. (2021)

Table 5. Cost balance equations and auxiliary equations of system components.

Component	Cost balance equations	Auxiliary equations
Collector	$c_{12} \cdot \dot{E}x_{12} + c_{solar} \cdot \dot{E}x_{solar} + \dot{Z}_{coll} = c_{13} \cdot \dot{E}x_{13}$	$c_{solar} = 0$
HEX	$c_{13} \cdot \dot{E}x_{13} + c_5 \cdot \dot{E}x_5 + \dot{Z}_{HEX} = c_{12} \cdot \dot{E}x_{12} + c_9 \cdot \dot{E}x_9$	$c_{12} = c_{13}$
Evaporator	$c_1 \cdot \dot{E}x_1 + c_4 \cdot \dot{E}x_4 + \dot{Z}_{evap} = c_2 \cdot \dot{E}x_2 + c_5 \cdot \dot{E}x_5$	$c_1 = c_2, c_1 = 0$
Turbine	$c_9 \cdot \dot{E}x_9 + \dot{Z}_{turb} = c_{10} \cdot \dot{E}x_{10} + c_{elec} \cdot \dot{W}_{turb}$	$c_9 = c_{10}$
Condenser	$c_{10} \cdot \dot{E}x_{10} + c_7 \cdot \dot{E}x_7 + \dot{Z}_{cond} = c_3 \cdot \dot{E}x_3 + c_{11} \cdot \dot{E}x_{11}$	$c_9 = c_3, c_7 = 0$
Pump	$c_3 \cdot \dot{E}x_3 + c_{elec} \cdot \dot{W}_{pump} + \dot{Z}_{pump} = c_4 \cdot \dot{E}x_4$	

Table 6. The result list of similar analysis studies in the literature survey.

Autor(s)	Product(s)	Source Temperature	Results
Zhou et al. [5]	•Electricity	90-210 °C	The hybrid plant annually produces 76.3%, 74.7%, and 62.7% more power than the stand-alone geothermal plant in Longreach, Moomba, and Renmark, respectively. Levelized cost of electricity for the hybrid plant was found to be about 23% less than that of the stand-alone geothermal plant (EGS) (i.e. 225 $/MWh).
Ayub et al. [6]	• Electricity	135 °C	According to design results, they determined 7% solar share of net power output. The analysis shows that LEC (levelized electricity cost) can be decreased by 2% for the hybrid compared to a stand-alone geothermal system. The constant-flow solar trough system offers 5.5% and the variable-flow solar trough system offers 6.3% higher power output compared to the sole geothermal system. (Ayub 2015)
Atiz et al. [7]	• Electricity	63-74-86 °C	It was determined that the selection of the working fluid affected the performance of the ORC. The maximum overall energy and exergy efficiencies of the system were calculated as to be 6.92% and 21.06% by using n-butane for the source in Turgutlu, respectively. The minimum overall energy and exergy efficiencies of the system were calculated as 0.32% and 2.19% by using n-hexane for the source in Kula.
Başoğul [9]	•Electricity	160-170 °C	The exergy efficiency was determined as 39.1% while the cost rate per unit of electricity produced by the GPP was 0.055 $/kWh.
Tozlu et al. [10]	•Electricity •Heating	100 °C	The average electricity production costs of PTC-ORC, PTC-CGN and PTC-HYB are found to be 0.257 $/kWh, 0.448 $/kWh and 0.401 $/kWh, respectively. The energy efficiencies of both systems are higher than the exergy efficiencies. The efficiencies of both systems show values below 10% when the storage is considered.
Sen and Yılmaz [11]	•Electricity • Cooling	130 °C	This geothermal and solar energy combined system has a 2720 kW cooling capacity and 2235 kW net power. The combined system's first and second law efficiencies are 19.6% and 43.7%. The unit cooling and electricity cost is 0.074 $/kWh (20.77 $/GJ) and 0.017 (4.71 $/GJ) $/kWh, respectively.

Guler et al. [12]	•Electricity • Heating • H_2 Production	130 °C	The exergy efficiencies of Model 1, Model 2 and Model 3 were determined as 32.1%, 32.4%, and 30.6%, respectively. The conversion electricity costs of fuel cells are calculated as 0.0792, 0.0781, and 0.0792 $/kW, respectively.

Figure List

Figure 1. The scheme and T-s diagrams of the solar-geothermal hybrid ORC system.

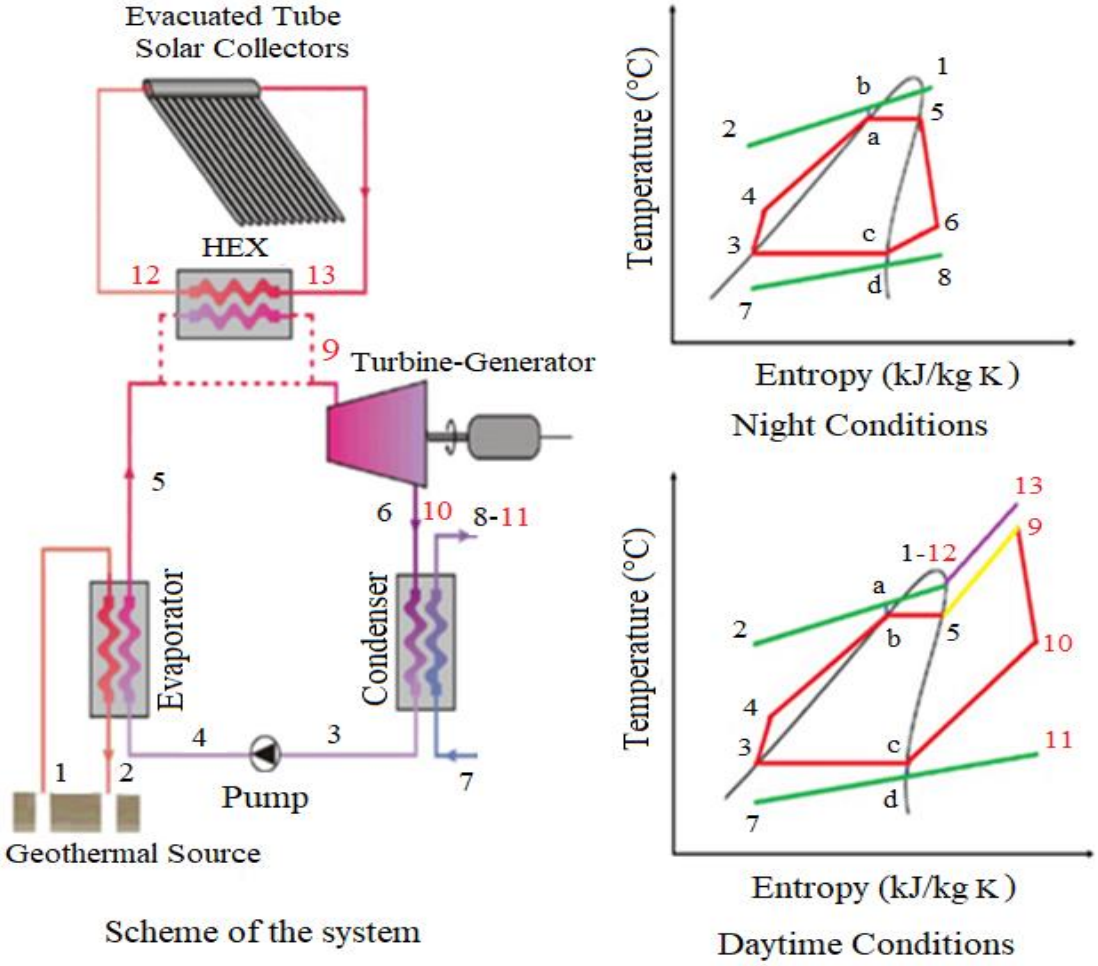

Figure 2. The variation of annual electricity generation of the system with the increase of geothermal source temperature.

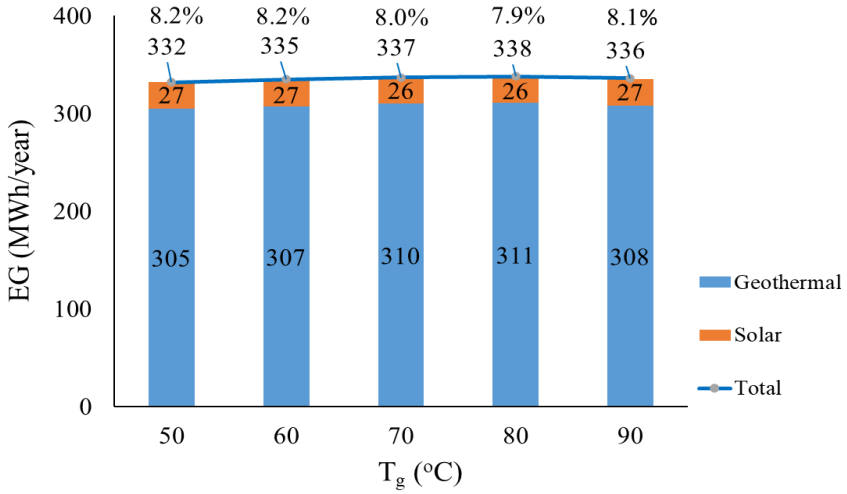

Figure 3. The variation of annual energy (η) and exergy (Ψ) efficiencies of the system with the increase of geothermal source temperature.

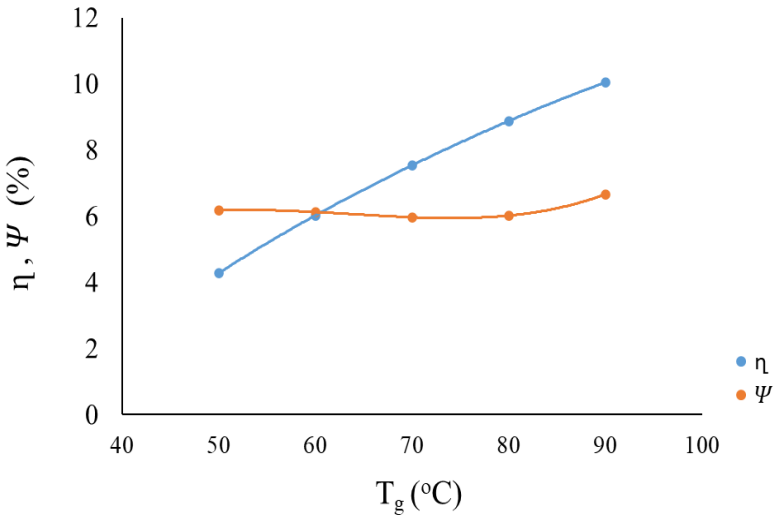

Figure 4. The variation of annual exergy destructions of the system components with the increase of geothermal source temperature.

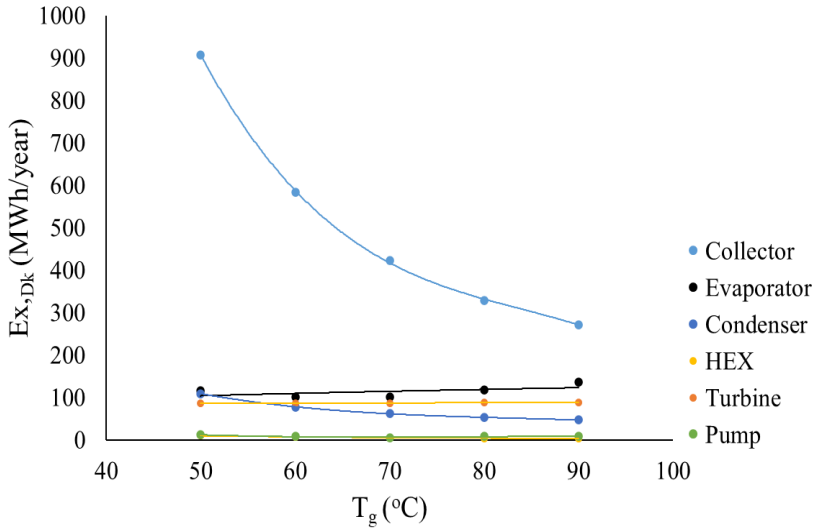

Figure 5. The variation of exergy efficiencies of system components with the increase of geothermal source temperature.

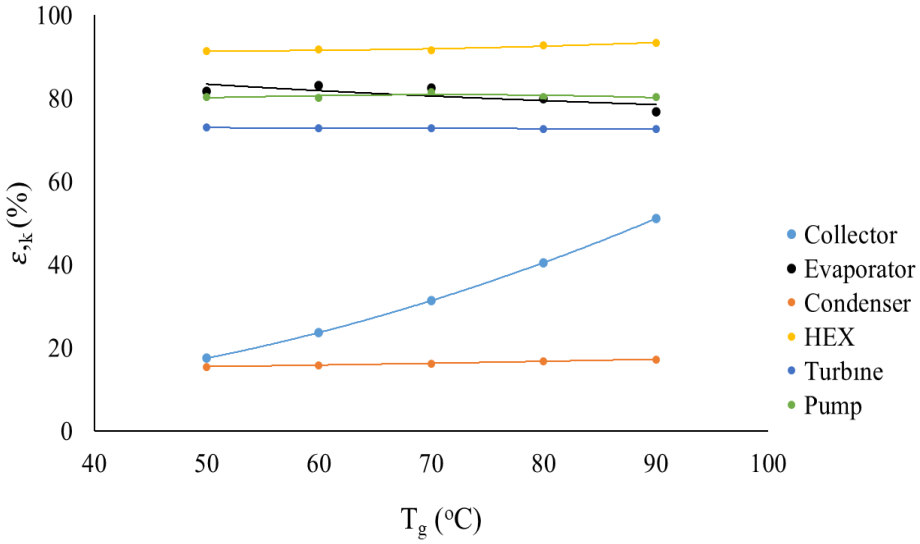

Figure 6. The variation annual exergy destruction cost rates of system components with the increase of geothermal source temperature.

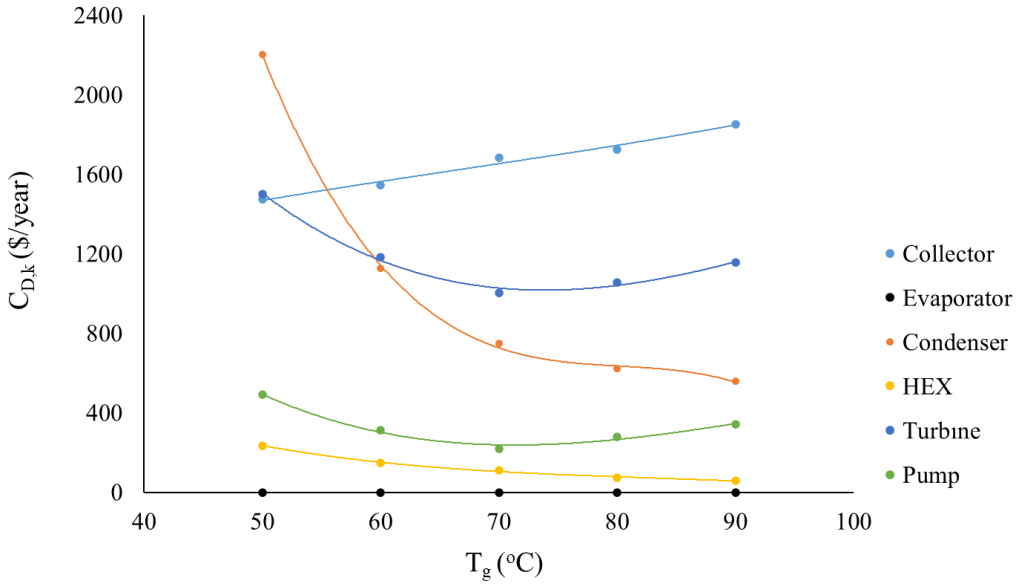

Figure 7. The variation exergoeconomic factors of system components with the increase of geothermal source temperature.

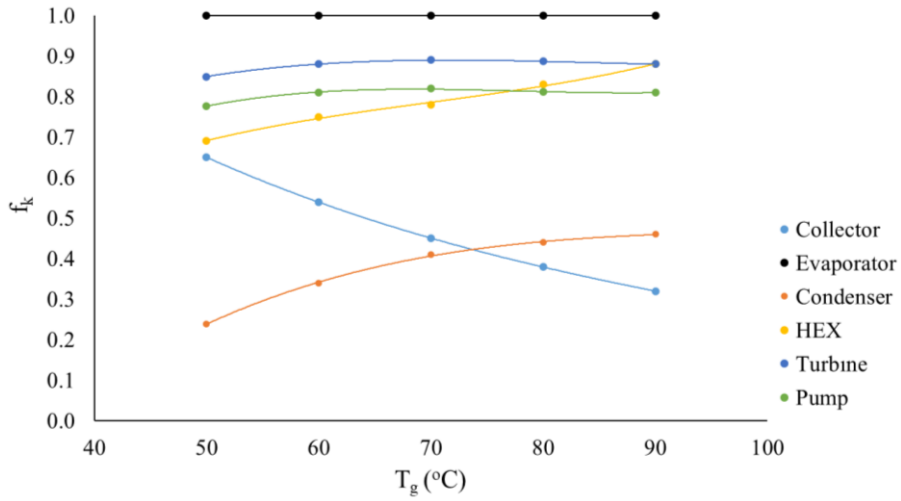

Figure 8. The variation electricity generation cost of the system with the increase of geothermal source temperature.

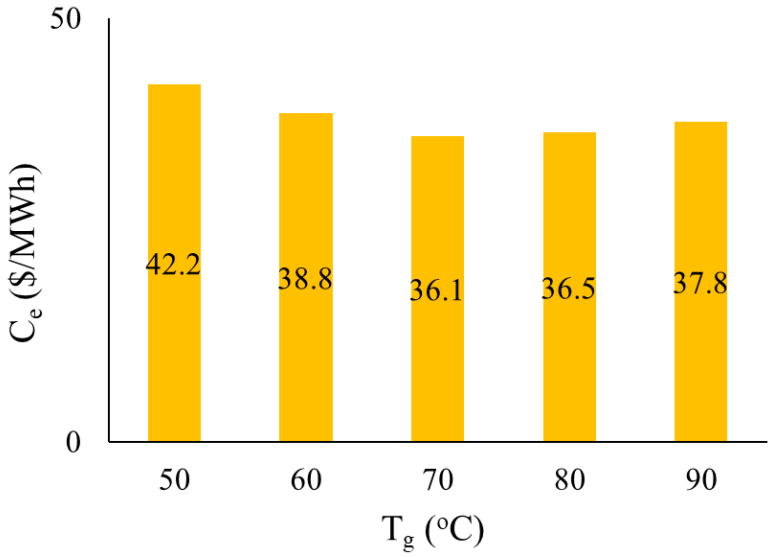

Biography

Fatih Akkurt graduated from the Department of Mechanical Engineering of İstanbul Technical University, Turkey in 1997. He obtained his MS degree and Ph. D from the Department of Mechanical Engineering of Selçuk University in 2003 and in 2012, respectively, He has been working as an Associate Professor at Necmettin Erbakan University in Konya since 2012. His main research interests include energy and exergy analysis of thermodynamic systems.

* *Corresponding author.*
E-mail address: fakkurt@erbakan.edu.tr